observations of the Sea 1 ce Cover Using Satellite Radar Interferometry

R. Kwok

Jet Propulsion -Laboratory
California Institute of Technology
4800 Oak Grove Drive
Pasadena, CA 91109

Submitted to *Geophysical Research Letters*

June 8, 1995

Please send correspondences to:

Dr. Ronald Kwok
Jet Propulsion laboratory
California Institute of Technology
MS 300-235
4800 Oak Grove Drive
Pasadena, CA 91109

Observations of the Sea Ice Cover Using Satellite Radar Interferometry

Ron ald Kwok

Jet Propulsion Laboratory
California Institute of Technology
4800 Oak Grove Drive
Pasadena, CA 91109

Abstract

The fringes observed in repeat pass interferograms are expressions of surface relief and relative displacements. The limiting condition in the application of spaceborne radar interferometry to the remote sensing of the sea ice cover is the the large magnitude of motion between repeat passes. The translation and rotation of ice floes tend to decorrelate the observations rendering radar interferometry ineffective. In our study, we have located three images in the high Arctic during a period when there was negligible motion between repeat observations. The fringes obtained from these images show a wealth of information about the sea ice cover which is important in atmosphere-ice interactions and sea ice mechanics. These measurements provide the first detailed remote sensing view of the sea ice cover. Ridges can be observed and their heights estimated if the interferometric baseline allows. We have observed ridges with heights greater than 4m. The variability in the phase measurements over an area provides an indication of the large scale roughness. Relative centimetric displacements between rigid ice floes have been observed. We illustrate these observations with examples extracted from the interferograms formed from this set of ERS - 1 SAR images.

1 Introduction

Repeat-pass radar interferometry provides the capability to observe the surface relief and centimetric displacements of the surface of interest. In sea ice, one of the parameters which affect the coupling of the atmosphere to the ice surface is the roughness of the surface at different scales *[overland,* 1985]. In particular, with large widely- spaced pressure ridges in the central Arctic, the roughness is also locally anisotropic due to the height, length and density of these ridges as w c]] as the orientation of these structures relative to the wind direction. A previous study by Burns [1 990] to relate Synthetic Aperture Radar (SAR) backscatter statistics to the atmospheric drag over sea ice indicated that the ridge areas in the pack icc needs to be quantified in terms of ridge frequency and ridge heights to be useful for indicating areas of different- drag coefficients. Although the radar backscatter is sensitive to the presense of ridges, there is no model to relate the intensity to ridge height or ridge density. We demonstrate that radar interferometry has the potential to provide direct observations the surface roughness statistics at the scale of the sensor resolution and structural description (e.g. orientation, frequency, height etc.) of ridges that arc greater than resolution elements of the radar. Surface topography is also correlated to bottom roughness.

An additional observation obtainable from repeat pass radar interferometry is centimetric (vertical or horizontal) relative displacements of the sea ice. These displacements could be duc to thermal cracks, tilts of ice surface, converging or diverging floes, We provide an example to illustrate the displacement of an icc floe as observed by radar interferometry. However, the physical interpretations of these observations are generally more difficult because of the lack of in-situ measurements at these scales and the ambiguities of the interferometric measurements. in this paper, we focus on the some of the issues associated with repeat-pass interferometry over sea icc and some of the interesting results obtained using the datasct described herein,

2 Repeat-Pass Radar Interferometry

The coordinate system and geometry for repeat-pass interferometry is depicted in Fig. 1. For a given set of repeat observations, from the ith and jth epochs, with baseline B_{ij} and look angle θ, the phase difference or interferometric phase at each sample is [*Zebker et al.*, 1994],

$$\Delta\phi_{ij} = 2kB_{ij}\sin(\theta - \alpha_{ij}) \tag{1}$$

where α is the tilt of the baseline with respect to the horizontal and k is the wavenumber of the radar. The phase convention we use here in complex notation is $e^{-j\Delta\phi}$ and we omit the negative sign in our equations. The difference in the slant range path length $(|\vec{r}_i| - |\vec{r}_j|)$ is approximated by $\vec{B}, \vec{r}$. This term contains phase contributions from the orientation of the Earth surface relative to the interferometric baseline. If the surface scatterers are displaced between observations then the observed phase will include a contribution of $2k\vec{d}\cdot\vec{r}$ due this displacement [*Massonnet et al.*, 1993], or

$$\Delta\phi_{ij} = 2kB_{ij}\sin(\theta - \alpha_{ij}) + 2k\Delta\rho \tag{2}$$

Here, we write $\vec{d}\cdot\vec{r}$ as $\Delta\rho$. This additional term is independent of the spatial baseline.

The baselines are usually decomposed into a component which is perpendicular to the line of sight or range direction $(B_\perp = B\cos(\theta - \alpha))$ and a component which is parallel to this direction $(B_\parallel = B\sin(\theta - \alpha))$. The sensitivity of the interferometer to surface relief is dependent only on the magnitude of the perpendicular separation. In repeat-pass interferometry, the baseline is defined by the physical separation in the observation locations. For sea ice, however, an additional component of baseline is introduced by ice motion in the range direction. We note here that interferometry is possible only if this effective baseline due to orbit separation and ice motion is less than this critical baseline such that coherence of the radar echoes is maintained. Additionally, the differential rotation and the surface changes of the sea ice cover have to be small [*Zebker and Villasenor*, 1992]. For ERS-1, complete decorrelation results when the baseline is greater than approximately 1 km and the rotation

angle is greater than 0.7°. These constraints limit the routine observations of the sea ice cover with repeat pass interferometry.

3 Data Analysis

Three ERS-1SAR images of sea ice, with observation intervals of 3-days, from January of 1992 were used in this analysis. These images were located off the Queen Elizabeth Islands at approximately 128.78°E and 80.140N, We selected this time period and this area for two reasons. During this time period, there was negligible ice motion in this area as indicated by the 3-day ice motion record derived by an image- based ice motion tracker operated at the Alaska SAR Facility [*Kwok et al.*, 1991]. This region is also interesting because of the ridge density and ridge height [*Wadhams*, 1981]; an area of intense ridging due to the convergence of ice causing extensive deformation of the ice cover. This is to ensure that the critical baseline is not exceeded and that the interferometer is sensitive to the surface features available in the datasct.

We formed the interferograms using a technique described in Gabriel and Goldstein [1 988]. Because there is negligible large scale relief on the sea ice surface, we estimate the effective baseline of the interferometer by assuming that we are observing a locally spherical surface of the Earth. A phase function due to this spherical surface was then removed such that the surface relief and displacements are emphasized. We estimate the effective interferometric baseline between the first and second repeat observations, B_{12}, to be 47 m. B_{23} and B_{13} were 297 m and 342 m, respectively. They vary slightly along track. The first and third observations are separated by six days.

To illustrate the features in the interferograms that are close to the resolution of the sensor, we focus on a 3 km x 4 km area (Fig. 2). The pixels sizes are 7.9 m in range and 4 m in azimuth, Figures 3 and 4 are the interferograms derived from the SAR datasets. The interferogram from the first and second observations is not shown or discussed here because

the interferometric baseline is not sensitive to the expected surface relief or height of ridges (typically less than 10 m).

4 Interpretation and Discussion

Each interferogram shows the phase shift at each pixel relative to the reference image. in our color coding scheme, a π phase shift is represented by a cycle of the color wheel (increasing in the direction from yellow-rcxl-blue-green-ycl]ow). The observed phase consists of contributions from the varying surface relief on the ice cover as well as the range component of the surface displacement during the repeat observation interval. As noted above, the fringe patterns duc to topography arc sensitive to the the baseline of the interferometer whereas those duc to range displacements arc not. For a typical ERS- 1 baseline of say 80m, the sensitivity to topography is approximately 32 m/radian. The sensitivity to displacement is higher. Half a wavelength of range displacement (2.8 cm for ERS- 1 radar wavelength of 5.6 cm) produces a phase shift of 27r. If wc assume no surface relief (or zero baseline), each fringe can be converted to a horizontal or vertical displacement.

Surface Relief

Of the two repeat pass interferometers, the one with the longer baseline (B_{13}) provides a sensitivity of approximately 8.6 m/radian whereas the shorter baseline one (B_{23}) provides a sensitivity of approximately 9.7 m/radian at the center of the image. Identical features can be found on both interferograms. Wc first discuss the surface relief on the ice floes where the arrows ident ify some of the common features on both interferograms. These features arc most likely due to ridges on the icc cover. Wc note here that these features are difficult to identify in the SAR intensity image data. The higher color contrast of these features in Fig. 3 is due to the longer baseline of the interferometer. The average heights of these three ridges can be calculated by estimating the phase difference between the peak (orallgc-red) of onc of these features to a reference surface (light-blue - Fig. 3). We estimate a phase of approximately

0.75 radians giving a average peak height of 6.5m. With the same procedure, we estimate an average peak height of 5.9 m of the same ridges from interferogram. The most likely cause of the discrepancy is due to the errors in the estimation of the baselines and phase noise of the interferometer. The peak elevation of these ridges are not unreasonable [Wadhams, 1981] although they should have a relatively low frequency of occurrence. In addition to the ridge heights, a number of other parameters to characterize the surface could be computed from the data. It seems that some structural description of ridges could be constructed (ridge height, ridge density and ridge orientation) although some of these parameters could be limited by the resolution and sensitivity of this particular radar and interferometer. A statistical description of the surface roughness at the spatial scales of the resolution element could be also computed. Figure 5 shows the interferometric phase distribution of the a 150x150 pixel area (fairly rough) around the top arrow. The distributions are centered at $\pi/2$. As expected, the standard deviations of the phase agree to a scale factor which is the ratio of the sensitivity of the interferometers. Conversion to height gives a standard deviation of approximately 1.95 m, which seems high. But we point out here that the phase noise of the interferometer in this case would give an uncertainty of 1.5 m comparable to that of this quantity. increasing the number of samples to estimate the mean phase would reduce the noise contribution but at the expense of spatial resolution.

We briefly note here that the surface relief floe on the right side (of Fig. 4) is fairly moderate compared to the floe where the arrows are located and also that there are ridges defining the boundaries of floes.

Displacements

We direct the reader's attention to the red ice floe in Fig. 3 and the same floe in Fig. 4. in Fig. 3, there is an average phase bias relative to the surrounding ice floes whereas this phase difference was not observed in Fig. 4. It is unlikely that this is due to surface relief because the ice floe would have to be meters above or below the adjacent floes to introduce this magnitude of phase difference. However, a vertical or horizontal displacement of the floe

between observations could easily introduce such an effect because of the interferometer's sensitivity to displacements. This phase difference indicates a line of sight displacement of the order of half a centimeter which translates into a possible vertical displacement of 0.46 cm or a horizontal displacement of 0.2 cm. The sign of the displacement is ambiguous and we cannot resolve the direction of motion because we are observing only the projection of the 3-dimensional displacement vector into the radar look direction. Since we observe a fairly flat phase field other than those due to surface relief (in Fig. 4), this movement of the sea ice occurred between the first and second observations and not between the second and third observations. We do not speculate on the physical cause of the displacement, suffice it is to point out that the interferometric measurements do indicate the existence of such phenomena in the sea ice and that radar interferometry could be used to measure small movements of sea ice. These movements could be due to small scale ridging, thermal or mechanical cracks, tilts of the ice surface or just response of the individual floes to ocean forcing.

5 Summary

Satellite radar interferometry offers the potential to map the sea ice cover in terms of surface topography and centimetric displacements. The observations presented here have provided the first detailed remote sensing view of the sea ice cover. Sea ice motion constrains the use of repeat-pass radar interferometry if the motion is large compared to the critical baseline of the interferometer. Additionally, the sensitivity of the interferometer needs to be high because of the scale of the surface relief. Interferometric observations of sea ice is therefore more suited to the ERS-1 and ERS-2 tandem phase type mission where the repeat interval is shorter. Certainly, if an operational interferometric mission were to be launched, the potential of detailed mapping of the sea ice cover should be considered.

Acknowledgments

R. Kwok performed this work at the Jet Propulsion]] laboratory, California Institute of

Technology under contract with the National Aeronautics and Space Administration.

References

Burns, B. A., SAR image statistics related to atmospheric drag over sea ice. *IEEE Trans. Geosci. Remote Sens.*, Vol, 28, No. 2, pp.1 58-165, 1 990.

Gabriel, A. 1<. and R. M. Goldstein, Crossed orbit interferometry: Theory and experimental results from SIR-B, *Int. J. of Remote Sens.*, Vol. 9, No. 8, pp. 857-872, 1988.

Kwok, 1{., J.C. Curlander, R. McConnell and S. Pang, An Ice Motion Tracking System at the Alaska SAR Facility, *IEEE J. of Oceanic Engineering,* Vol. 15, No. 1, 44-54, 1990.

Massonnet, 1)., M. Rossi, C. Carmona, F. Adraga, G. Peltzer, 1<. Feigi and '1'. Rabaute, The displacement field of the Landers earthquake mapped by radar interferometry, *Nature, vo]. 364, pp.* 138-142, 1993.

Overland, J, E. Atmospheric boundary layer structu e and drag coefficients over sea ice. *J. Geophys. Res.*, Vol. 90, No. C5, 9029-9049, 1985.

Wadhams, 1'., Sca ice topography of the Arctic Ocean in the region 70W to 25E. *Phil. Trans. Royal Sot, London, A* (302):45-85, *1981.*

Zebker, 11, A., C. 1,. Werner, l). A. Rosen, S. Hensley, Accuracy of topographic maps derived from ERS- 1 interferometric radar, *IEEE Trans. Geosci. Remote Sens.*, Vol, *32,* pp. *823-836,* 1994.

Zebker, H. A. and J. Villasenor, Decorrelation in interferometric radar cc1 1oc s, *IEEE Trans. Geosci. Remote Sens.*, Vol. *30,* pp. *950-959, 1 992.*

Figure Captions

Figure **1,** Interferometer imaging configuration. A baseline, B, is created between the ith and jth repeat observations of the same ground area, At an almost identical look angle of θ, the differential range to a point on the ground is given by the interferometric phase. α is the tilt of the baseline relative to the horizontal.

Figure 2. ERS-1SAR image of sea ice off the Queen Elizabeth Islands. (Location: 128.78°E, 80.14°N) (©ESA 1994).

Figure 3. Interferogram formed from the first and third observations. Arrows identify some of the features which are common to both interferograms.

Figure 4. Interferogram formed from the second and third observations.

Figure 5. Interferometric phase distribution of an area (1 50x1 50 pixels) around arrow number 1, (a) PDF from the interferogram in Fig. 3. (b) PDF from the interferogram in Fig. 4.

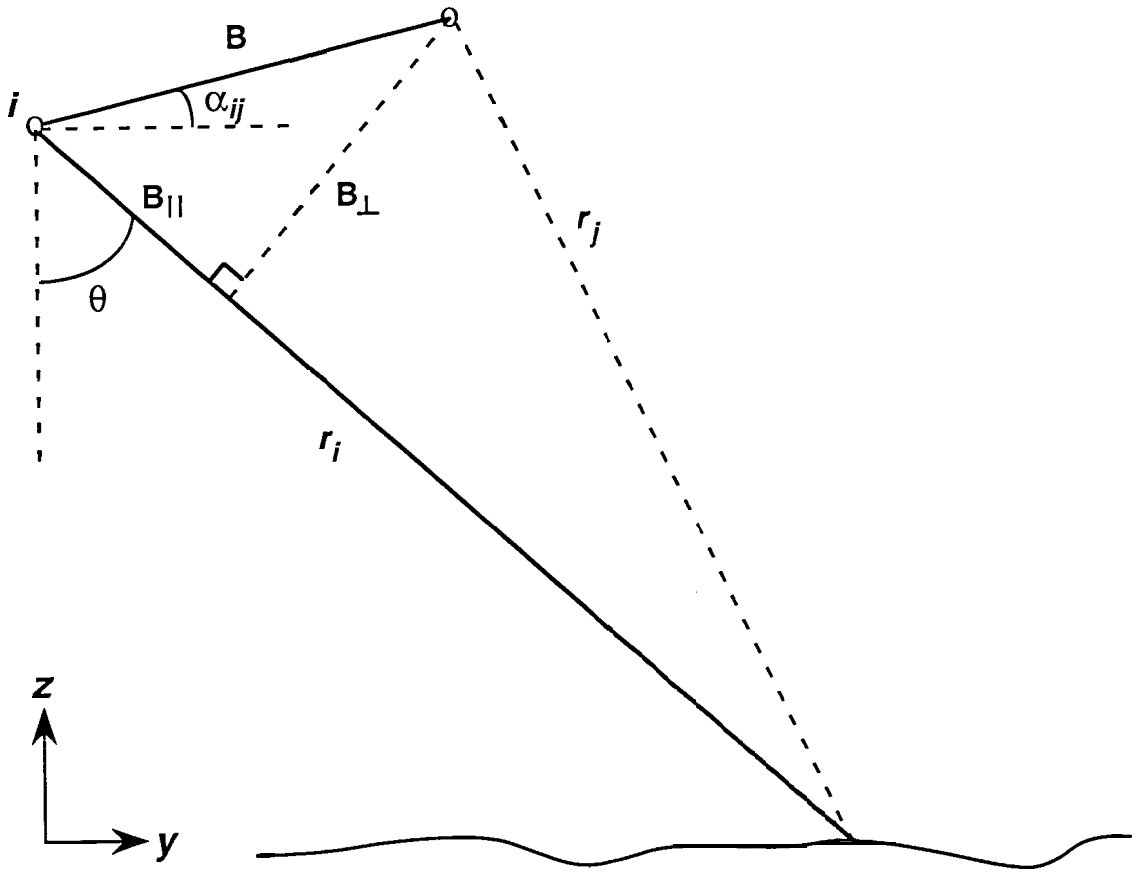

Fig. 1

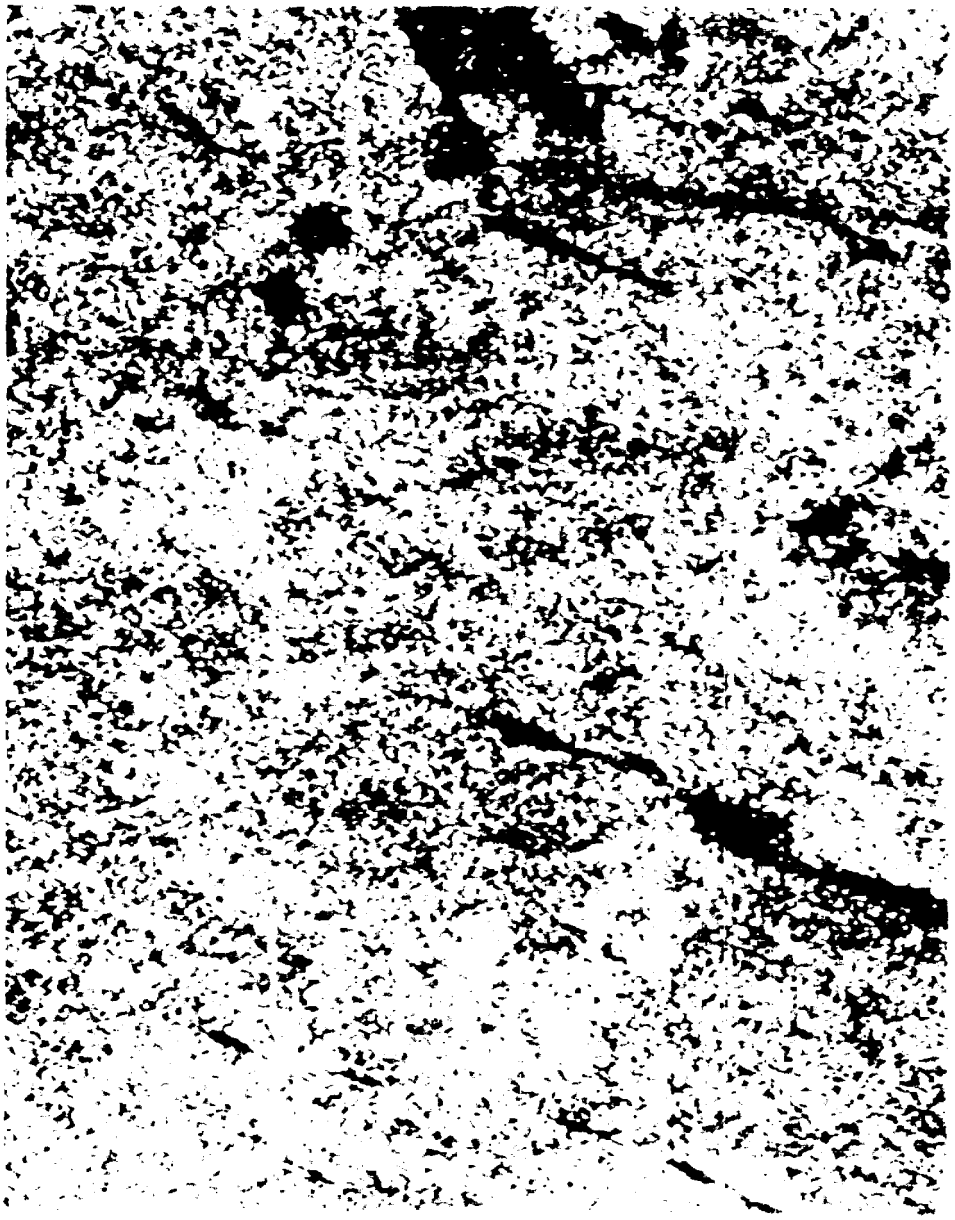

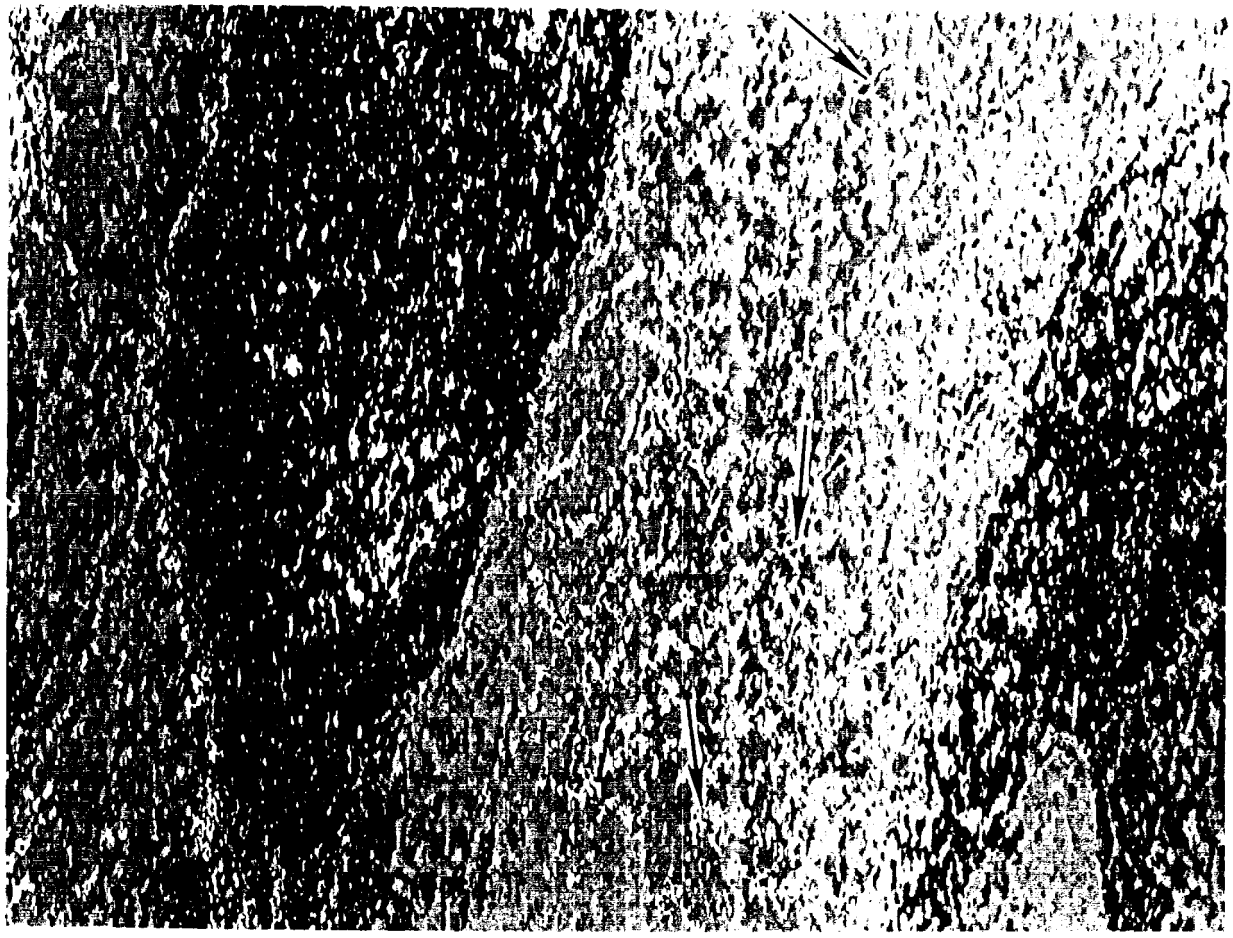

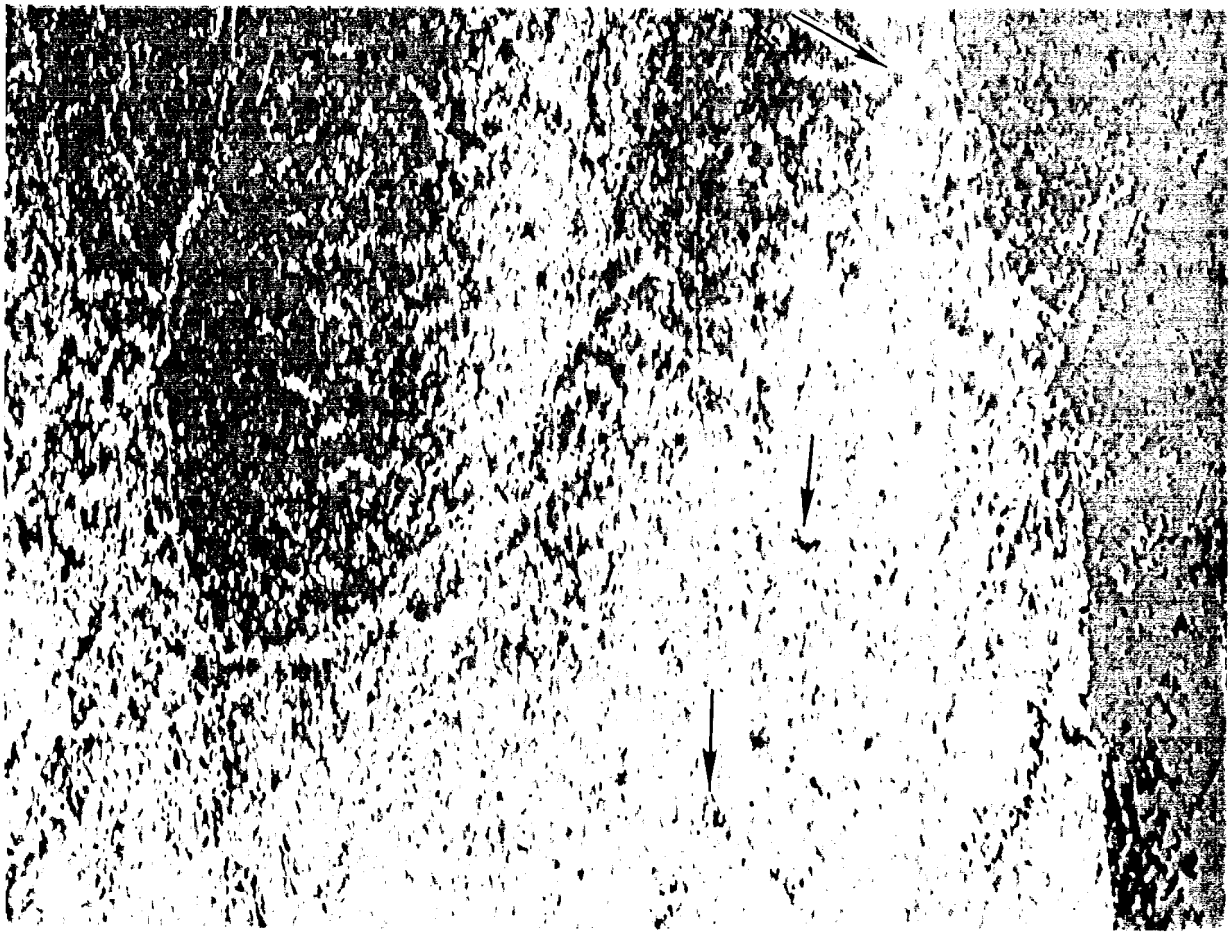

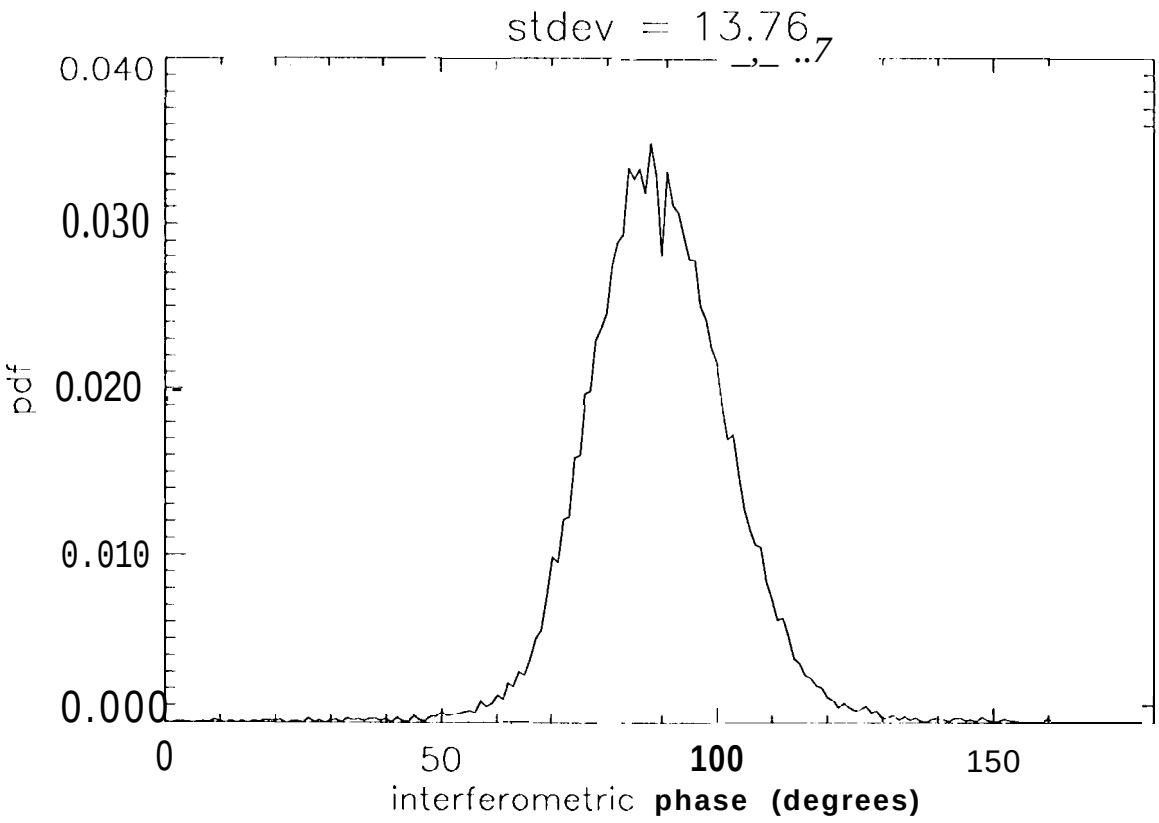
stdev = 13.76
0.040
0.030
0.020
0.010
0.000
pdf
0
50
100
150
interferometric phase (degrees)

(a)

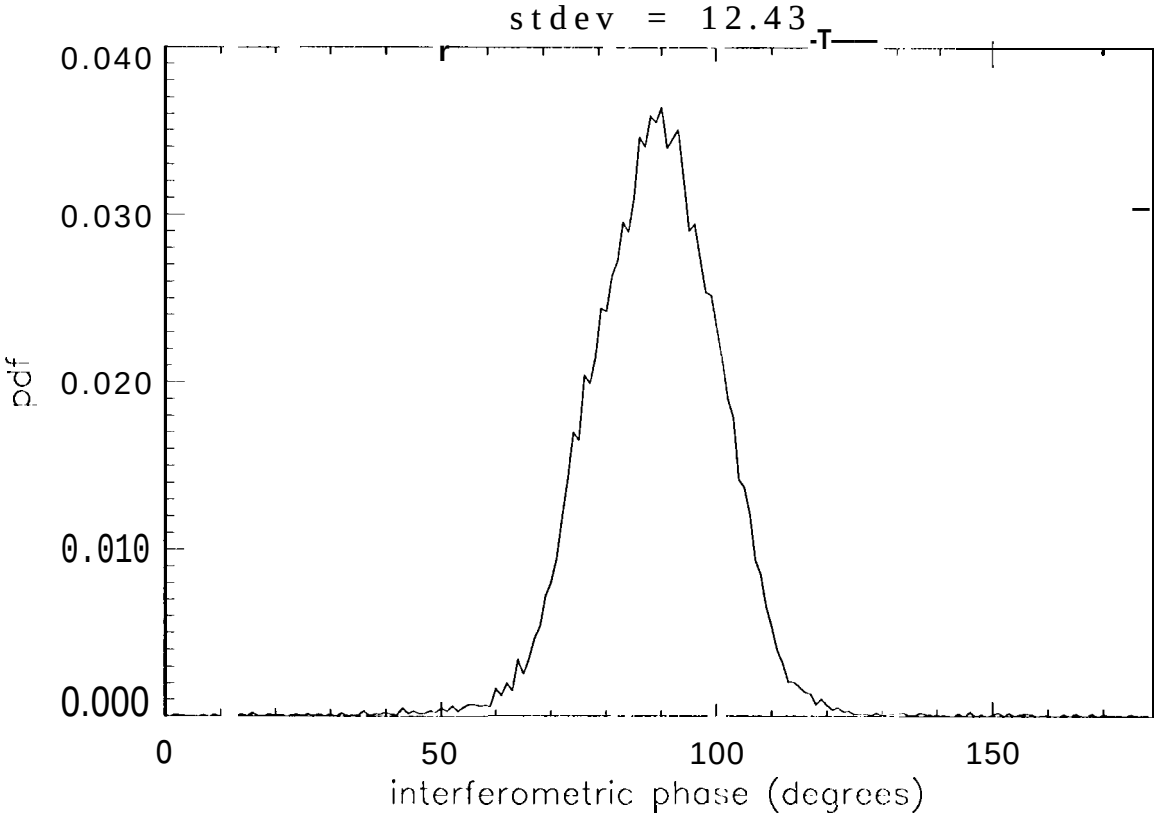
stdev = 12.43
0.040
0.030
0.020
0.010
0.000
pdf
0
50
100
150
interferometric phase (degrees)

(b)